Journal of Organometallic Chemistry, 330 (1987) 85–100
Elsevier Sequoia S.A., Lausanne – Printed in The Netherlands

Mono- and di-hydrido-bridged platinum(II)-tungsten(IV) complexes. Synthesis and X-ray crystal structure of $[Cp_2W(\mu\text{-}H)_2PtPh(PEt_3)][BPh_4]$ and $[Cp_2(H)W(\mu\text{-}H)PtPh(PEt_3)_2][BPh_4]$ *

Alberto Albinati, Ralph Naegeli,

Istituto di Chimica Farmaceutica dell'Università di Milano, Viale Abruzzi 42, I-20131 Milano (Italy)

Antonio Togni and Luigi M. Venanzi*

Laboratorium für Anorganische Chemie, ETHZ, Universitätstrasse 6, CH-8092 Zürich (Switzerland)

(Received December 19th, 1986)

Abstract

The preparation of compounds $[Cp_2HW(\mu\text{-}H)PtR(PEt_3)_2]X$ (R = H, Ph, **7**; X = BF_4, BPh_4) and $[Cp_2W(\mu\text{-}H)_2PtR(PEt_3)][BPh_4]$ (**10**), is reported. The X-ray crystal structures of **7**[BPh_4] and **10**[BPh_4] were determined. The crystals of the former are triclinic, space group $P\bar{1}$, a 11.146(3), b 19.841(3), c 22.301(4) Å, α 88.09(1), β 87.92(2), γ 76.36(2)°, V 4787.5 Å^3 and $Z = 4$. The crystals of the latter are triclinic, space group $P\bar{1}$, a 15.759(4), b 14.045(3), c 9.467(2) Å, α 89.92(2), β 107.04(2), γ 88.98(2)°, V 2004.3 Å^3, $Z = 2$.

Introduction

It is well-known [1] that weakly coordinating ligands, e.g., solvent molecules, in complexes of the type $[M(solvent)_mL_n]$ can be easily replaced by other two-electron donors in a reaction of the type:

$$[M(solvent)_mL_n] + mL' \rightarrow [ML'_mL_n] + m \text{ solvent} \quad (1)$$

It has also been frequently observed [2] that coordinated solvent molecules can be displaced by transition metal hydride complexes with the formation of M–H–M bond assemblies:

$$[M(solvent)_mL_n] + [M'H_mL'_p] \rightarrow [L_nM(\mu\text{-}H)_mM'L'_p] + m \text{ solvent} \quad (2)$$

* Dedicated to Professor L. Sacconi in recognition of his important contribution to organometallic chemistry.

It was, therefore, of interest to investigate the reaction of solvento complexes with transition metal hydrides that are also known to act as two-electron donors and to establish whether in such cases, reaction 1 would be favoured over reaction 2 or vice-versa.

For this purpose $[WH_2Cp_2]$ (**1**) ($Cp = \eta^5\text{-}C_5H_5$) [3] was chosen as the hydride since it has been reported to be both a base and a nucleophile [4]. In this study the solvento cations *trans*-$[PtR(solvent)(PEt_3)_2]^+$ (**2**, R = H; **3**, R = Ph) were used, since they are known to react both with two-electron donors according to reaction 1 [1] as well as with transition metal hydrides according to reaction 2 [2]. Examples of the latter type of behaviour are provided by compounds **4** and **5**, which contain Pt–H–Pt moieties and can be prepared from reactions 3 and 4 respectively:

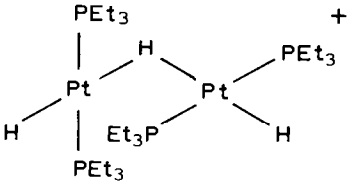

(4)

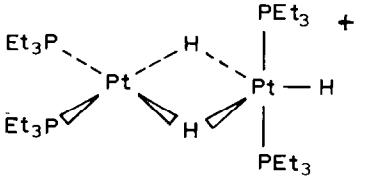

(5)

$$trans\text{-}[PtH_2(PEt_3)_2] + trans\text{-}[PtH(MeOH)(PEt_3)_2]^+ \rightarrow \mathbf{4} + MeOH \quad (3)$$

$$cis\text{-}[PtH_2(PEt_3)_2] + trans\text{-}[PtH(MeOH)(PEt_3)_2]^+ \rightarrow \mathbf{5} + MeOH \quad (4)$$

This paper describes the products of the reactions of **1** with **2** or **3** and their subsequent transformations. A preliminary account has appeared elsewhere [5].

Results and discussion

Hydride **1** reacts with cations **2** or **3** as shown in Scheme 1. The binuclear products **6** and **7** are obtained by adding pre-cooled solutions of cations **2** and **3**, respectively (solvent = MeOH or acetone), in the corresponding solvents, to pre-cooled toluene solutions of **1**. Complex formation is fast even at −78 °C. The reddish-brown $[BF_4]$ salts of the bimetallic cations **6** and **7**, which can be obtained in crystalline form directly from the reaction solutions, are then used for the analytical and spectroscopic characterization.

The WH_2Cp_2 unit in complexes **6** and **7** is very weakly bound and easily displaced by ligands such as PEt_3 and CO, as shown in equation 5.

$$\mathbf{6} + L \rightarrow \mathbf{1} + trans\text{-}[PtRL(PEt_3)_2]^+ \quad (5)$$

(**8a**, R = H; L = PEt_3;
8b, R = H; L = CO;
9a, R = Ph; L = PEt_3;
9b, R = Ph; L = CO)

The lability of complexes **6** and **7** is also confirmed by the observations that (a) the ^1H NMR spectrum of **6**, dissolved in THF-d_8, corresponds to that expected for the static structure only below ca. −105 °C, and (b) the hydride ligands bonded to

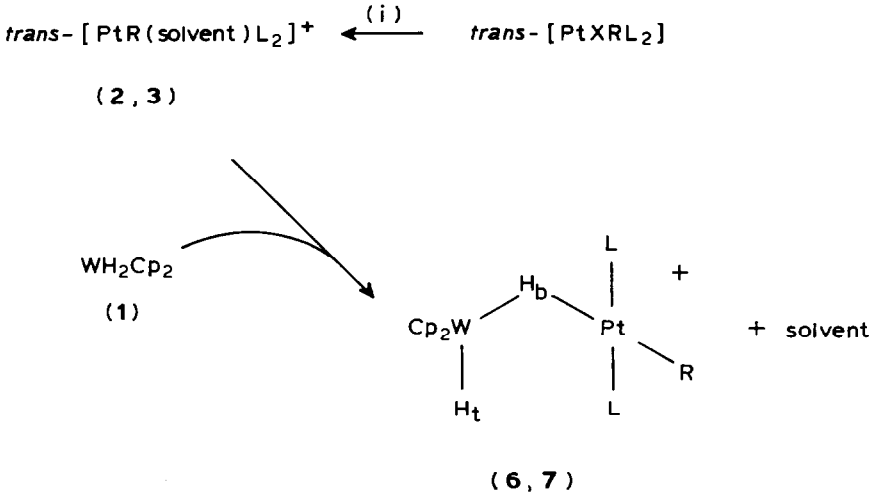

Scheme 1. X = Cl, I; R = H (**6**), R = Ph (**7**); L = PEt_3; (i) $AgBF_4$ in acetone or methanol followed by filtration of AgX.

Table 1

^1H and $^{31}P\{H\}$ NMR parameters for the cations **6**, **7** and **10** [a]

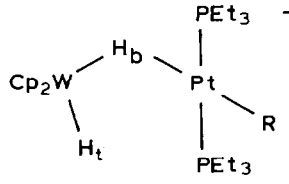

(**6**, R = H_t [b]; **7**, R = Ph [b])

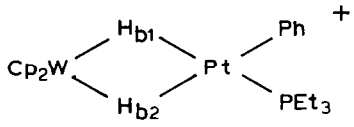

(**10**)

	6	**7**	**10**
$\delta(H_{b1})$			−14.1
$\delta(H_{b2})$	−15.6	−18.7	−17.1
$\delta(H_t)$	−12.7	–	–
$^1J(W,H_{b1})$			99.1
$^1J(W,H_{b2})$	60.3	59.7	101.1
$^1J(Pt,H_{b1})$			727.0
$^1J(Pt,H_{b2})$	200.8	192.3	625.0
$^1J(Pt,H_t)$	1334.7	–	–
$^2J(P,H_{b1})$			59.6
$^2J(P,H_{b2})$	9.6	3.7	8.8
$^2J(P,H_t)$	27.9	–	–
δ(Cp)	4.78	4.95	5.16
$\delta(^{31}P)$	15.1	8.4	28.6
^1J(Pt,P)	2611.3	2735.6	3397.4

[a] CD_2Cl_2 solutions; parameters calculated from spectra run at −30 °C for compounds **6** and **7** and at −48 °C for **10**; coupling constants in Hz. [b] The two hydride ligands are spectroscopically indistinguishable as they are interchanging (see Results and discussion).

tungsten undergo a H/D exchange reaction when **6** is dissolved in acetone-d_6. Thus, one hour after a solution of **6** in acetone-d_6 has been made up at room temperature, signals are observed that are assignable to the three isotopomers containing the units: WH_2PtH, **6**-d_0, WHDPtH, **6**-d_1, WD_2PtH, **6**-d_2. (The formulation **6**-d_1 denotes the dynamic equivalent of the two static structures HW(μ-D)PtH and DW(μ-H)PtH. In this context it should be noted that the H-atom bonded only to platinum does not undergo H/D exchange.) This exchange is likely to involve dissociation of **6** with liberation of **1**, which is known to undergo hydrogen/deuterium exchange with protonic solvents [6]. It is noteworthy that isotope-effects are observed on the chemical shifts of both the H(Pt) and ^{31}P resonances (see Table 1).

Treatment of one equivalent of $[WH_2Cp_2]$ (**1**) with two equivalents of $[PtPh(acetone)(PEt_3)_2]^+$ (**3**) gives $[PtPh(PEt_3)_3]^+$ (**9a**) [7] and the new complex cation $[Cp_2W(\mu\text{-}H)_2PtPh(PEt_3)]^+$ (**10**). This cation can also be obtained by addition

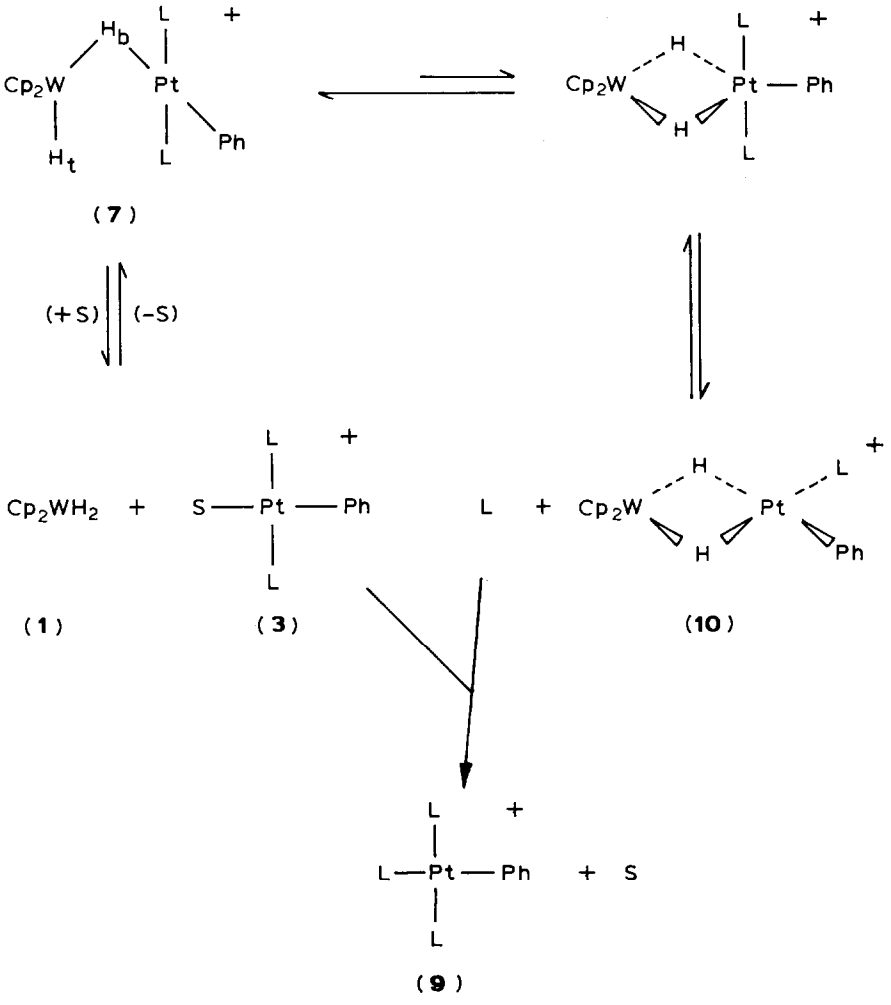

Scheme 2. L = PEt_3; S = acetone.

of one equivalent of the solvento complex **3a** to the bimetallic complex **7**. These equilibria are summarized in Scheme 2.

In an attempt to assist the dissociation of a phosphine, the monohydrido-bridged complex **7** was treated with half an equivalent of $[(P^nBu_3)ClPt(\mu\text{-}Cl)_2PtCl(P^nBu_3)]$ (**11**), which is known to react with phosphines to give *cis*- and/or *trans*-$[PtCl_2(PEt_3)(P^nBu_3)]$ (**12**) [8]. ^{31}P NMR spectroscopic examination of the resulting deep-brown solution showed the presence of at least three products, of which only *trans*-$[PtClPh(PEt_3)_2]$ (**13**) could be identified; neither **12** nor **10** were present in this solution. Since **1** alone reacts with **11** to give a complex mixture of products, it is likely that the expected phosphine-abstraction reaction is prevented by the prior reaction of **1** with **11**. Thus, the conversion of **7** into **10** requires reagents which do not react with $[WH_2Cp_2]$ (**1**). It is noteworthy that when **10** is treated with one equivalent of PEt_3, in addition to the expected monohydrido-bridged species, **7**, a significant amount of the tris-phosphine cation $[PtPh(PEt_3)_3]^+$ (**9a**) is formed, accompanied by the corresponding amount of **1**. This reaction indicates that partial bridge opening (k_1) and the addition of a second phosphine (k_2) to platinum occur

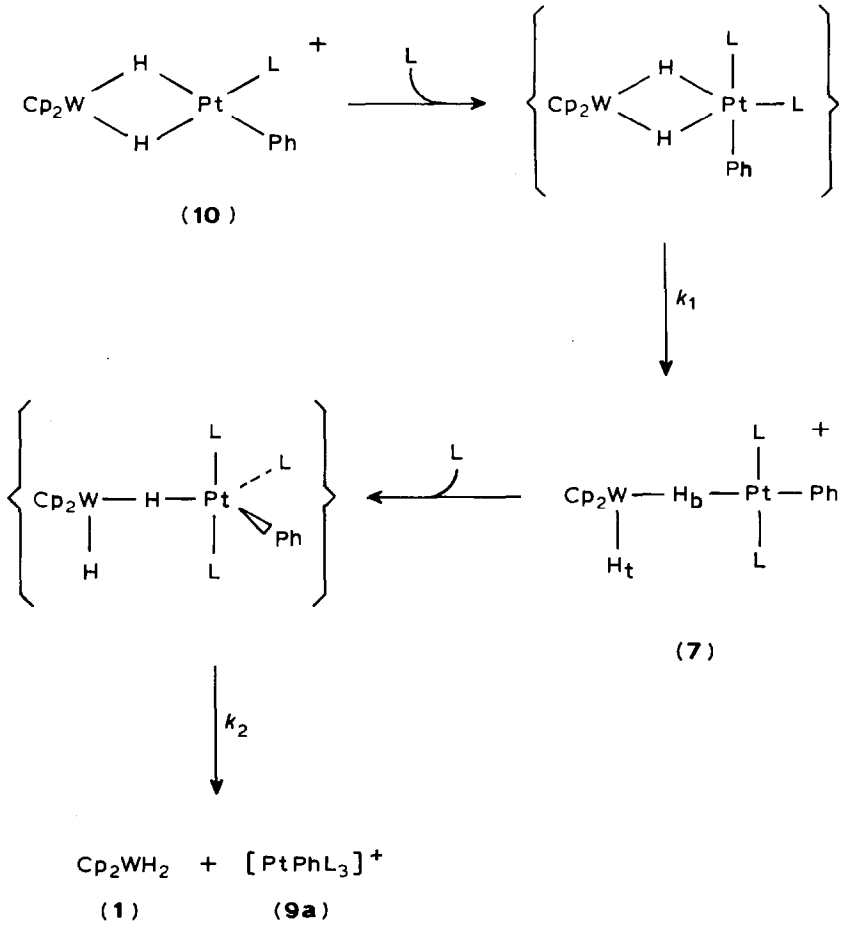

Scheme 3. L = PEt_3.

at comparable rates. A possible mechanistic pathway for these reactions is shown in Scheme 3.

NMR spectroscopic characterization of 6, 7 and 10

A summary of the NMR parameters for the hydrido-bridged complexes **6**, **7** and **10** is given in Table 1.

The ^1H NMR spectrum of **6** at $-30\,^\circ C$ shows two groups of resonances in the ratio 1/2, due to H_t and the two hydrogens interacting with both metals, respectively. The lower field signal has a triplet structure arising from coupling to the equivalent phosphorus atoms (as can be demonstrated under ^{31}P-selective decoupling conditions) and shows Pt-satellites. No other couplings are observed. The higher field resonance, i.e., that due to the hydrides interacting with both metals, shows couplings to P, Pt and W. A very similar type of resonance is found in **7**.

The interesting parameters for both compounds are $^1J(^{195}Pt, ^1H)$ and $^1J(^{183}W, ^1H)$: the observed values of $^1J(^{195}Pt, ^1H_b)$ of 200.8 and 192.3 Hz, for **6** and **7**, respectively, are rather small, and can be viewed as an average between a large $^1J(^{195}Pt, ^1H)$ and a small $^3J(^{195}Pt, ^1H)$, if it is assumed that only one hydride is bridging (the second being terminal on tungsten) and that there is a very rapid exchange on the NMR time scale i.e., $J(^{195}Pt, ^1H) \approx \frac{1}{2}(^3J(^{195}Pt, ^1H) + ^1J(^{195}Pt, ^1H))$.

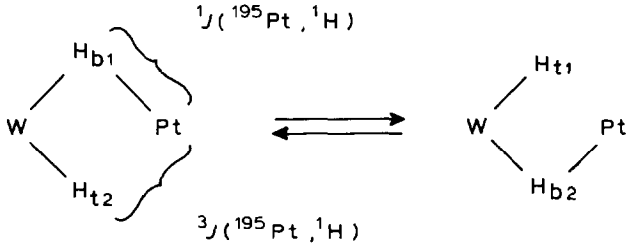

This assumption is supported by a study of the temperature dependence of the spectrum of **7** in THF-d_8. Broadening of the signals is observed in the range -40–$80\,^\circ C$. Although at about $-80\,^\circ C$ coalescence occurs, no other significant change takes place on lowering of the temperature to ca. $-100\,^\circ C$; thus, no activation parameters for this process could be obtained.

The values of $^1J(^{183}W, ^1H)$ for **6** and **7** are lower than that for Cp_2WH_2 ($^1J(^{183}W, ^1H)$ 72.3 Hz) and are comparable with those found for compounds formed by addition of a Lewis-acid to **1** *.

The ^1H NMR spectrum of **10** is also temperature dependent. The single, very broad high field resonance observed at room temperature coalesces at ca. $+7\,^\circ C$, and sharp signals with resolved structure are observed in the range -15–$75\,^\circ C$. At ca. $-40\,^\circ C$ the high field region of the spectrum is characterized by the presence of two doublets (integrals 1/1) arising from the couplings of the two non-equivalent hydride ligands with the unique P-atom. The lower-field doublet shows the largest coupling and is therefore assigned to H_{b1}, *trans* to the PEt_3 ligand. Both hydrides are coupled to the metals. The values of $^1J(^{195}Pt, ^1H)$ of 727 and 625 Hz, respec-

* $^1J(^{183}W, ^1H)$ in e.g. $WH_2Cp_2 \cdot Mo(CO)_5$ is 63 Hz [11].

tively, are quite large in comparison with the values found for Pt-hydrido bridged complexes of the type $[(R_3P)_2Pt(\mu\text{-}H)_2PtR'(PR_3)_2]^+$ [12] or $[(Et_3P)_2ArPt(\mu\text{-}H)PtAr'(PEt_3)_2]^+$ [13], which fall in the ranges 300–606 Hz and 443–448 Hz, respectively. These large values can be taken as indicative of strong interaction in the bridging moiety. Similar remarks can be made about the $^1J(^{183}W, ^1H)$ coupling constants (of 99.1 and 101.1 Hz, respectively). These fall in a range observed for the structurally related complexes $[Cp_2W(\mu\text{-}H)_2Rh(PPh_3)_2]^+$ ($^1J(^{183}W, ^1H)$ 107 Hz) [14] and $[CpW(\mu\text{-}H)_2(\mu\text{-}(\eta^5:\eta^1\text{-}C_5H_4)IrH(PEt_3)_2]^+$ ($^1J(^{183}W, ^1H)$ 92.4 and 95.2 Hz) [15]. Interestingly, no coupling between H_{b1} and H_{b2} could be resolved; given the observed line-widths, $^2J(H_{b1}, H_{b2})$ must be less than 5 Hz.

The $^{31}P\{^1H\}$ spectra of the three complexes **6**, **7** and **10** are characterized by a single resonance with Pt-satellites. No $^{183}W, ^{31}P$ couplings were observed for either compound.

Noteworthy is the large down field shift ($\Delta\delta \approx +20$ ppm) of the ^{31}P resonance and the increase of about 360 Hz of $^1J(^{195}Pt, ^{31}P)$ on going from **7** to **10**, indicating a much stronger Pt–P interaction in **10**. In view of the dynamic equivalence, on the NMR time scale, of the hydride ligands that interact with both metal centers in **6** and **7**, the ^{31}P NMR spectra were recorded under "off-resonance" conditions; as

Table 2

Selected bond lengths (Å) and angles (deg) for cation **7**

	Mol. 1	Mol 2
Pt–W	3.501(1)	3.440(1)
Pt–P(1)	2.337(5)	2.331(5)
Pt–P(2)	2.332(5)	2.328(5)
Pt–C(1)	2.03(1)	2.04(2)
W–Cp(1) [a]	1.95(2)	1.96(2)
W–Cp(2) [a]	1.94(2)	1.95(2)
P(1)–C [b]	1.85(2)	1.84(3)
P(2)–C [b]	1.84(2)	1.83(2)
(C–C)Cp [b]	1.44(5)	1.43(5)
Pt–W–Cp(1) [a]	101.2(2)	110.1(3)
Pt–W–Cp(2) [a]	112.1(2)	104.1(2)
Cp(1)–W–Cp(2) [a]	143.4(5)	143.8(7)
W–Pt–P(1)	90.4(1)	90.2(1)
W–Pt–P(2)	97.9(1)	97.1(1)
W–Pt–C(1)	169.0(2)	173.5(2)
P(1)–Pt–P(2)	170.6(4)	171.6(4)
P(1)–Pt–C(1)	87.6(5)	88.6(5)
P(2)–Pt–C(1)	85.0(5)	84.6(5)
Pt–P(1)–C(1)	113.0(5)	115.3(6)
Pt–P(1)–C(3)	117.0(5)	117.2(6)
Pt–P(1)–C(5)	113.7(6)	110.3(6)
Pt–P(2)–C(1)	114.8(5)	115.6(5)
Pt–P(2)–C(3)	115.0(6)	115.2(6)
Pt–P(2)–C(5)	113.0(6)	115.0(5)

[a] Cp(1) and Cp(2) refer to the centers of gravity of the cyclopentadienyl groups. [b] Average values; the standard deviation of the mean is obtained from the formula $s(d) = [\Sigma_i(d_i - d)^2/(n-1)]^{1/2}$, where n is the number of observations.

expected the single signal (the satellites being neglected) is split into a doublet of triplets for **6** and into a triplet for **7**, respectively, thus confirming the postulated structures of those complexes.

The X-ray crystal structures of $7[BPh_4]$ and $10[BPh_4]$

These have been discussed in some detail previously [5] and only a few additional points will be made here. As stated previously, the main features of these structures are:

(1) In both complexes the tungsten atom is pseudo-tetrahedrally coordinated to the two Cp rings and the two hydride ligands, one of them terminal and the other bridging.

(2) In both complexes the platinum atom adopts a square planar coordination which, in **7**, comprises a bridging hydride ligand, a phenyl carbon atom, and two phosphorus atoms, while in **10** the four donor atoms are two bridging hydride ligands, one phenyl carbon atom, and one phosphorus atom.

The approximate positions of the hydride ligands in both complexes were obtained by potential energy minimization using the HYDEX programme (see Experimental Section). ORTEP drawings of the cations **7** and **10** are shown in Fig. 1 and 2, respectively. Selected bond lengths and angles are shown in Tables 2 and 3, respectively.

As pointed out previously [5], the most significant difference between the two compounds is the W–Pt distance which is ca. 3.5 Å in **7** but only ca. 2.7 Å in **10**.

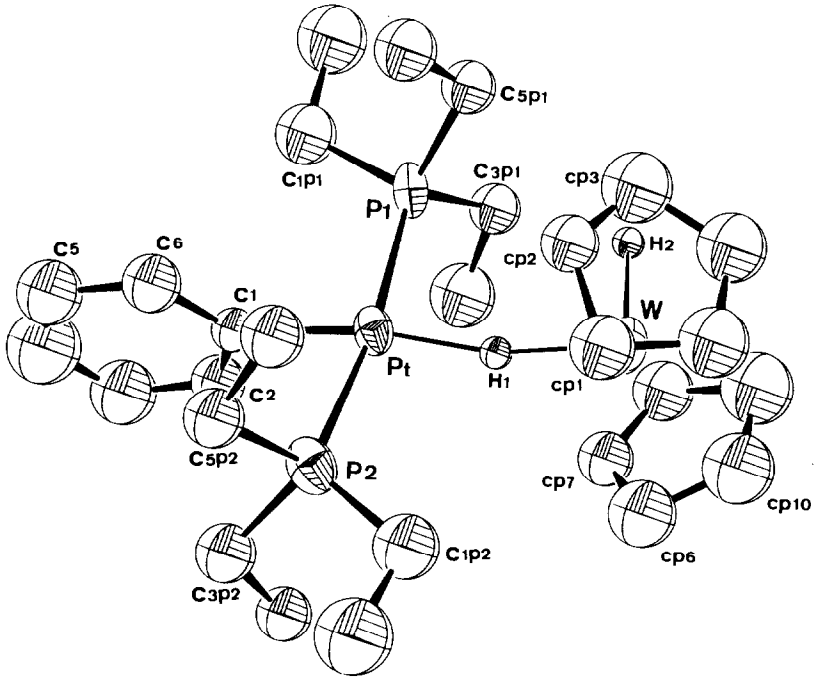

Fig. 1. An ORTEP view of $[(\eta^5\text{-}C_5H_5)_2HW(\mu\text{-}H)Pt(Ph)(PEt_3)_2]^+$ (**7**).

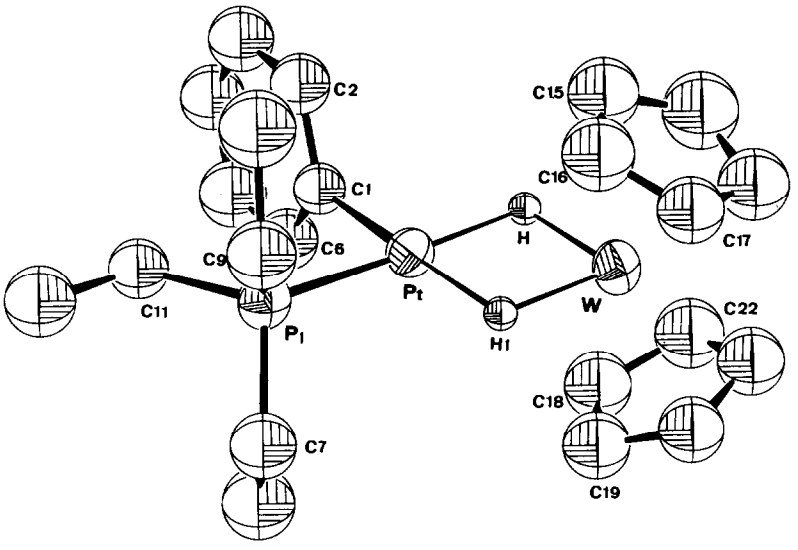

Fig. 2. An ORTEP view of $[(\eta^5\text{-}C_5H_5)_2W(\mu\text{-}H)_2Pt(Ph)(PEt_3)]^+$ (**10**).

While the latter value is typical of $M(\mu\text{-}H)_2M'$ assemblies [16], the former is significantly longer than the average value for $M(\mu\text{-}H)M'$ assemblies [17]. It is noteworthy that it is comparable with the W–W distance (3.528(2) Å) in

Table 3

Selected bond lengths (Å), angles and torsion angles (deg) for cation **10**

W–Pt	2.663(1)	Pt–W–Cp(1) [a]	108.5(6)
Pt–P(1)	2.215(5)	Pt–W–Cp(2) [a]	110.6(6)
Pt–C(1)	2.01(1)	Cp(1)–W–Cp(2) [a]	141.0(8)
W–Cp(1) [a]	1.94(2)	Pt–P(1)–C(7)	111.5(6)
W–Cp(2) [a]	1.98(1)	Pt–P(1)–C(9)	110.2(6)
P(1)–C(7)	1.82(2)	Pt–P(1)–C(11)	119.8(4)
P(1)–C(9)	1.83(2)	P(1)–Pt–C(1)	88.2(5)
P(1)–C(11)	1.80(2)	W–Pt–C(1)	134.0(2)
$C\text{–}C_{Ph}$ [b]	1.38(6)	W–Pt–P(1)	137.8(1)
C(13)–C(14)	1.42(3)	C(1)–C(2)–C(3)	123.0(1.1)
C(14)–C(15)	1.36(3)	C(1)–C(6)–C(5)	120.3(1.2)
C(15)–C(16)	1.39(3)	C(2)–C(3)–C(4)	118.5(1.4)
C(16)–C(17)	1.39(3)	C(2)–C(1)–C(6)	116.6(1.2)
C(17)–C(13)	1.41(3)	C(3)–C(4)–C(5)	122.7(1.4)
C(18)–C(19)	1.35(3)	C(4)–C(5)–C(6)	118.5(1.3)
C(19)–C(20)	1.37(3)	C(7)–P(1)–C(9)	101.0(8)
C(20)–C(21)	1.37(3)	C(7)–P(1)–C(11)	107.1(8)
C(21)–C(22)	1.42(3)	C(9)–P(1)–C(11)	105.5(8)
C(22)–C(18)	1.34(3)	W–Pt–C(1)–C(2)	90.9
		W–Pt–P(1)–C(7)	53.5
		W–Pt–P(1)–C(9)	−57.8
		W–Pt–P(1)–C(11)	179.5

[a] Cp(1) and Cp(2) denote the centers of gravity of the two cyclopentadienyl groups. [b] Average values; the standard deviation of the mean is calculated according to $s(d) = [\Sigma_i(d_i - d)^2/(n-1)]^{1/2}$, where n is the number of observations. [c] Standard deviations on the torsion angles are in the range 0.9–1.3°.

$[NEt_4][(CO)_5W(\mu\text{-}H)W(CO)_5]$ [17], a compound in which the W–H–W interaction is so weak that the W–W distance changes significantly with a change of counter-ion; e.g., it is 3.391(1) Å in its $[(Ph_3P)_2N]^+$ salt [17]. It can also be deduced that the W–H–Pt interaction in **7** is weak, and this is confirmed by the observation that the metal–metal distance in the two independent molecules in the unit cell differ by 0.06 Å (see Table 2).

Finally, it is noteworthy that the shorter Pt–P distance in **10** than in **7** is consistent with the larger value of the $^1J(^{195}Pt, ^{31}P)$ coupling constants for the former compound (see Table 1).

Experimental section

Synthesis

All operations were carried out under purified nitrogen using standard Schlenk techniques. Solvents were dried and distilled under nitrogen prior to use. Elemental analyses were performed by the Microanalytical Section of the Swiss Federal Institute of Technology. ^1H, ^{31}P and ^{195}Pt NMR spectra were recorded at 90 and/or 250.132, 36.43 and/or 101.21 and at 50.5 MHz, respectively, on Bruker FT WH90 and Bruker WM250 instruments. ^1H, ^{31}P and ^{195}Pt chemical shifts are given relative to external TMS, 85% H_3PO_4 and Na_2PtCl_6, respectively. Positive values denote shifts downfield from the reference. Infrared spectra were recorded on an Beckman 4250 spectrophotometer as KBr pellets or Nujol mulls.

The compounds $[WH_2Cp_2]$ [3], *trans*-$[PtHCl(PEt_3)_2]$ [18], $[Pt(PEt_3)_3]$ [19] and *sym-trans*-$[Pt_2Cl_4(PBu^n_3)_2]$ [20] were prepared by published methods, whereas *trans*-$[PtXPh(PEt_3)_2]$ (X = Cl, I) were synthesized by oxidative addition of PhX to $[Pt(PEt_3)_3]$ in a modification of the procedure reported by Parshall [21] for the preparation of *trans*-$[PtXAr(PEt_3)_2]$ from ArX and $[Pt(PEt_3)_4]$.

$[Cp_2HW(\mu\text{-}H)PtPh(PEt_3)_2]BX_4$ (7[BX_4]: (X = F, Ph). 199 mg of crystalline *trans*-$[PtClPh(PEt_3)_2]$ (0.36 mmol) were added in small portions to a solution of 71 mg of $AgBF_4$ (0.36 mmol) in 20 ml of acetone. After 2 h stirring at room temperature AgCl was filtered off to leave an almost colorless clear solution of the solvated cation $[PtPh(PEt_3)_2]^+$. This was cooled to −78°C and slowly added to a cold (−78°C) solution of 120 mg of $[WH_2Cp_2]$ (0.38 mmol) in 30 ml of toluene with vigorous stirring. The red-brown mixture was stirred for 2 h at dry-ice temperature, then allowed to warm to room temperature. The solvent was evaporated under reduced pressure until the product, **7**[BF_4] separated as a brownish microcrystalline solid. This was filtered off, washed with toluene, diethyl ether, and pentane, and dried under vacuum (246 mg, 75%). Found: C, 36.81; H, 5.23. $C_{28}H_{47}P_2PtWBF_4$ calcd.: C, 36.90; H, 5.20%. Crystals of **7**[BPh_4] suitable for the X-ray study were obtained by dissolving 30 mg of **7**[BF_4] in 2 ml CH_2Cl_2, adding a solution of 1 equivalent of Na[BPh_4] in 5 ml MeOH, and allowing slow crystallization at 7°C.

$[Cp_2HW(\mu\text{-}H)PtH(PEt_3)_2]BF_4$ (6[BF_4]). This compound was prepared in a similar way to **7**[BF_4] but from $AgBF_4$, *trans*-$[PtHCl(PEt_3)_2]$ and $[WH_2Cp_2]$. Found: C, 32.48; H, 5.31. $C_{22}H_{43}P_2PtWBF_4$ calcd.: C, 31.64; H, 5.19%.

$[Cp_2W(\mu\text{-}H)_2PtPh(PEt_3)][BPh_4]$ (10[BPh_4]). A solution of 63 mg of $[WH_2Cp_2]$ (0.2 mmol) in 20 ml of acetone were added dropwise at room-temperature to an acetone solution of 0.4 mmol of *trans*-$[PtPh(acetone)(PEt_3)_2]^+$ (formed from the

reaction between 254 mg *trans*-[PtIPh(PEt_3)$_2$] and 78 mg $AgBF_4$). The mixture was stirred for 3 h, during which the color changed from yellow to red-brown to violet. The solution was concentrated under reduced pressure then added to a solution of 75 mg of $NaBPh_4$ (0.22 mmol) in 10 ml of MeOH. Cooling to −20 °C led to crystallisation of the product, which was filtered off, washed twice with 5 ml of methanol then diethyl ether and pentane, and dried in vacuum. Yield 144 mg (35% ref. to Pt). Violet prismatic crystals for the X-ray study were obtained by recrystallizing the compound from a 4/1 $MeOH/CH_2Cl_2$ mixture at ca. 7 °C. Found: C, 53.75; H, 5.29. $C_{46}H_{52}BPPtW$ calcd.: C, 53.98; H, 4.92%.

The second major product of the reaction, namely [PtPh(PEt_3)$_3$][BF_4] ([**9a**]BF_4), was inequivocably identified in the mother liquor by comparison of its ^{31}P NMR spectrum with that of an authentic sample.

Reactions

Reaction of ***10*** *with* PEt_3. A slight excess of PEt_3 (3.7 μl; 0.025 mmol) was added at room temperature to a solution of 25 mg [**10**][BPh_4] (0.024 mmol) in 1 ml CD_2Cl_2 contained in a serum-capped 5 mm NMR tube; the color of the solution changed instantaneously from violet to brown-red, showing that reaction was rapid. ^1H and ^{31}P NMR spectra were recorded at −48 °C and allowed the identification of

Table 4

Crystal data and data collection parameters for compounds **7**[BPh_4] and **10**[BPh_4]

Compound	**7**[BPh_4]	**10**[BPh_4]
Formula	$C_{52}H_{57}WPtBP_2$	$C_{46}H_{52}WPtBP$
Formula weight	1143.81	1025.65
Space group	$P\bar{1}$	$P\bar{1}$
a (Å)	11.146(3)	15.759(4)
b	19.841(3)	14.045(3)
c	22.301(4)	9.467(2)
α (deg)	88.09(1)	89.92(2)
β	87.92(2)	107.04(2)
γ	76.36(2)	88.98(2)
V (Å^3)	4787.5	2004.3
Z	4	2
D_{calc} (g cm^{-3})	1.586	1.699
Radiation	Mo-K_α graphite monochromated λ 0.71069 Å	
μ (cm^{-1})	54.74	65.11
θ range (deg)	$2.0 \leqslant \theta \leqslant 19.0$	$2.0 \leqslant \theta \leqslant 25.0$
Scan mode	$\omega/2\theta$	$\omega/2\theta$
Scan speed (deg s^{-1})	0.05	0.05
Scan width (deg)	1.10	1.10
Total bckgd time (s)	12	10
Receiving aperture (hor.vert.deg)	1.0–1.0	1.0–1.0
No. of data collected	7727 ($\pm h$, $\pm k$, $+l$)	8375 ($\pm h$, $\pm k$, $+l$)
No. of observed data ($I_{net} \geqslant 3\sigma(I)$)	6235	5452
R [a]	0.057	0.055
R_w [b]	0.060	0.069

[a] $\Sigma\|\Delta F\|/\Sigma|F_o|$ for observed reflections. [b] $(\Sigma|\Delta F|^2/\Sigma w|F_o|^2)^{1/2}$.

Table 5

Final positional and isotropic thermal parameters (B_{eq} and B_{iso}) for $[(\eta^5\text{-}C_5H_5)_2HW(\mu\text{-}H)Pt(Ph)(PEt_3)_2]^+$ (7) [a]

	x	y	z	B_{eq}/B_{iso}
Pt	0.29543(7)	0.26676(4)	−0.01992(3)	3.02 [a]
W	0.38873(7)	0.16292(4)	0.10763(3)	3.23 [a]
P(1)	0.10541(44)	0.31426(24)	0.02721(22)	3.26 [a]
P(2)	0.46747(48)	0.22326(25)	−0.08160(23)	3.56 [a]
C(1)P(1)	0.02084(175)	0.24857(100)	0.05154(84)	4.17(41)
C(2)P(1)	0.00533(227)	0.20323(130)	−0.00100(109)	6.79(58)
C(3)P(1)	0.10837(176)	0.36282(100)	0.09688(85)	4.19(42)
C(4)P(1)	0.15878(205)	0.42843(116)	0.08344(99)	5.65(51)
C(5)P(1)	−0.00326(186)	0.37588(106)	−0.02145(90)	4.71(45)
C(6)P(1)	−0.13116(215)	0.40714(123)	0.01238(103)	6.17(54)
C(1)P(2)	0.56859(178)	0.28180(102)	−0.09581(86)	4.31(43)
C(2)P(2)	0.63436(205)	0.29537(117)	−0.03917(98)	5.67(51)
C(3)P(2)	0.56744(189)	0.13892(107)	−0.05541(90)	4.78(45)
C(4)P(2)	0.68314(214)	0.11264(122)	−0.09640(103)	6.16(54)
C(5)P(2)	0.42673(199)	0.20605(112)	−0.15759(95)	5.29(48)
C(6)P(2)	0.34467(247)	0.15165(140)	−0.15715(118)	7.71(64)
Cp(1)	0.55776(186)	0.20925(106)	0.10544(89)	4.74(45)
Cp(2)	0.44936(185)	0.26657(105)	0.11313(89)	4.68(45)
Cp(3)	0.39211(198)	0.25754(113)	0.16818(96)	5.29(48)
Cp(4)	0.45461(204)	0.19439(116)	0.19657(98)	5.58(50)
Cp(5)	0.55882(194)	0.16517(111)	0.15704(93)	5.13(47)
Cp(6)	0.25637(202)	0.08686(115)	0.10159(98)	5.49(50)
Cp(7)	0.33902(204)	0.07038(115)	0.15203(97)	5.53(50)
Cp(8)	0.46724(185)	0.04984(105)	0.12930(89)	4.67(44)
Cp(9)	0.45772(188)	0.05771(108)	0.06235(91)	4.84(45)
Cp(10)	0.33219(204)	0.08008(115)	0.05144(98)	5.52(50)
C(1)	0.24996(168)	0.34145(96)	−0.08465(81)	3.76(39)
C(2)	0.29362(160)	0.40137(91)	−0.08191(76)	3.31(37)
C(3)	0.26400(201)	0.45757(115)	−0.12443(96)	5.46(49)
C(4)	0.19110(230)	0.44857(129)	−0.17223(109)	6.78(59)
C(5)	0.14500(203)	0.38992(116)	−0.17814(98)	5.60(50)
C(6)	0.17926(188)	0.33401(108)	−0.13268(90)	4.81(45)
Pt′	0.21553(7)	0.24248(4)	0.50528(3)	2.88 [a]
W′	−0.08772(8)	0.28860(4)	0.46401(4)	3.95 [a]
P(1′)	0.18517(51)	0.17960(26)	0.59220(24)	3.93 [a]
P(2′)	0.27441(44)	0.29437(25)	0.41761(23)	3.41 [a]
C(1)P(1′)	0.02796(225)	0.18426(128)	0.61714(107)	6.51(56)
C(2)P(1′)	0.01434(246)	0.13870(141)	0.67562(120)	7.68(65)
C(3)P(1′)	0.26714(209)	0.19793(119)	0.65958(101)	5.80(51)
C(4)P(1′)	0.20898(272)	0.27137(157)	0.68252(131)	9.14(75)
C(5)P(1′)	0.26017(201)	0.08694(114)	0.58373(97)	5.42(49)
C(6)P(1′)	0.20411(292)	0.05640(165)	0.52867(140)	9.93(81)
C(1)P(2′)	0.21310(177)	0.38816(101)	0.40996(86)	4.22(42)
C(2)P(2′)	0.23994(219)	0.42464(125)	0.46571(105)	6.36(55)
C(3)P(2′)	0.44101(205)	0.28501(116)	0.40618(98)	5.65(51)
C(4)P(2′)	0.47673(244)	0.31796(139)	0.34567(118)	7.50(64)
C(5)P(2′)	0.22604(178)	0.26283(101)	0.34800(86)	4.36(43)
C(6)P(2′)	0.27210(206)	0.18243(117)	0.34334(99)	5.64(50)
Cp(1′)	−0.06640(221)	0.22289(125)	0.37725(106)	6.39(55)
Cp(2′)	−0.19336(232)	0.25527(132)	0.38909(111)	6.92(59)

Table 5 (continued)

	x	y	z	B_{eq}/B_{iso}
Cp(3′)	−0.22934(218)	0.22868(125)	0.44667(106)	6.33(55)
Cp(4′)	−0.12746(199)	0.18059(113)	0.46945(95)	5.34(48)
Cp(5′)	−0.02919(223)	0.17796(127)	0.42288(107)	6.54(57)
Cp(6′)	−0.08875(248)	0.40425(141)	0.48169(119)	7.97(65)
Cp(7′)	−0.21241(225)	0.39576(128)	0.46211(108)	6.59(57)
Cp(8′)	−0.25343(236)	0.35682(134)	0.50967(114)	7.18(61)
Cp(9′)	−0.16583(224)	0.33479(128)	0.55402(108)	6.63(57)
Cp(10′)	−0.06858(232)	0.36909(132)	0.53626(112)	7.07(60)
C(1′)	0.39297(162)	0.22648(91)	0.53276(77)	3.41(37)
C(2′)	0.42612(178)	0.27702(102)	0.56668(86)	4.34(43)
C(3′)	0.54302(224)	0.26249(129)	0.59279(108)	6.57(57)
C(4′)	0.62516(239)	0.19859(137)	0.58326(115)	7.20(62)
C(5′)	0.59970(219)	0.14826(126)	0.54842(106)	6.24(55)
C(6′)	0.47577(193)	0.16245(109)	0.52238(93)	5.08(47)

[a] B_{eq} are given in the form $B = \frac{1}{3}(B_{11} + B_{22} + B_{33})$ [23]. Primed atoms refer to the second independent molecule in the cell.

1, **7**, **9a** and **10**. Some NMR parameters for **9a** are as follows: δ(H) −6.08 ppm; ^1J(Pt,H) 787.1 Hz; $^2J(P^{trans},H)$ 158.5 Hz; $^2J(P^{cis},H)$ 16.7 Hz.

Reaction of 7 with trans-[PtPh(acetone)(PEt$_3$)$_2$]$^+$ (3). A mixture of 60 mg [**7**][BF_4] (0.066 mmol) and 0.07 mmol *trans*-[PtPh(acetone)(PEt_3)$_2$][BF_4], ([**3**][BF_4]) in 15 ml acetone was kept at room temperature for 2 h. The solution was then taken to dryness under reduced pressure and the solid residue dissolved in 1 ml CD_2Cl_2. The ^{1}H and ^{31}P NMR spectra of this concentrated solution showed the presence of **10** and **9a** along with some unchanged **7** and **3**.

Reactions of 6 and 7 with PEt$_3$ and CO. Solutions of **6** or **7** in acetone were treated with either PEt_3 or CO and the products, **1**, **8a**, **8b**, **9a** and **9b** were identified by ^{1}H and ^{31}P NMR spectroscopy.

Crystallography

A Philips PW 1100 automatic diffractometer was used for both space group and cell constants determination and for data collection at room temperature. Crystallographic data and relevant details of the data collection are given for both compounds in Table 4. Data were corrected for Lorentz and polarization factors and an empirical absorption correction was applied using azimuthal ψ scans of 3 reflections having high χ angles. Intensities were considered as observed if $I_{net} \geq 3\sigma(I_{tot})$. The structures were solved by combined use of Patterson and Fourier methods and refined by block-diagonal least-squares using a Cruickshank weighting scheme [22]. The function minimized was $\Sigma w(|F_o| - 1/k|F_c|)^2$. No extinction correction was found to be necessary for either set of data. The scattering factors used were taken from ref. 9, and a correction for the real part of the anomalous dispersion was also taken into account [9].

Structural study of [7][BPh$_4$]

Crystals of [**7**][BPh_4] are prismatic and are air-stable. For data collection a crystal of approximate dimensions 0.16 × 0.31 × 0.35 mm was mounted on a glass fiber at a random orientation. Cell constants were obtained by least-squares fit of 25

Table 6

Final positional and isotropic thermal parameters (B_{eq} and B_{iso}) for $[(\eta^5\text{-}C_5H_5)_2W(\mu\text{-}H)_2Pt(Ph)(PEt_3)]^+$ (**10**) [a]

	x	y	z	B_{eq}/B_{iso}
Pt	0.30431(4)	0.23905(4)	0.27610(6)	3.10 [a]
W	0.12917(4)	0.24235(5)	0.22903(7)	3.32 [a]
P(1)	0.39886(27)	0.25253(31)	0.14443(45)	3.72 [a])
C(1)	0.40917(97)	0.22483(103)	0.45736(167)	3.77(30)
C(2)	0.44762(118)	0.13948(125)	0.50907(201)	5.41(39)
C(3)	0.51696(137)	0.12942(143)	0.64099(232)	6.76(46)
C(4)	0.54506(127)	0.20575(133)	0.71912(220)	6.16(43)
C(5)	0.51043(130)	0.29338(136)	0.67752(221)	6.20(43)
C(6)	0.43804(113)	0.30288(119)	0.54593(193)	5.01(37)
C(7)	0.37766(127)	0.36140(134)	0.03312(216)	6.04(42)
C(8)	0.39515(146)	0.45089(151)	0.13352(248)	7.40(51)
C(9)	0.37758(122)	0.16171(129)	0.00025(210)	5.74(40)
C(10)	0.39595(143)	0.05950(150)	0.06231(242)	7.25(50)
C(11)	0.51634(110)	0.24549(117)	0.23496(189)	4.85(36)
C(12)	0.57581(135)	0.25965(141)	0.13705(229)	6.66(46)
C(13)	0.01498(131)	0.14418(138)	0.20250(223)	6.34(44)
C(14)	0.04621(123)	0.13121(130)	0.07772(211)	5.85(41)
C(15)	0.12969(128)	0.09178(136)	0.11930(219)	6.21(43)
C(16)	0.15126(132)	0.08209(139)	0.27151(224)	6.38(44)
C(17)	0.08296(138)	0.11265(146)	0.32751(237)	6.92(48)
C(18)	0.05151(125)	0.37120(131)	0.10132(213)	5.86(41)
C(19)	0.13444(139)	0.40139(145)	0.16838(236)	6.87(47)
C(20)	0.15258(137)	0.39566(144)	0.31841(236)	6.79(47)
C(21)	0.07826(154)	0.36149(162)	0.34768(263)	7.96(55)
C(22)	0.01564(138)	0.34617(144)	0.20709(235)	6.80(47)

[a] For definitions see Table 5.

high order reflections using the PW 1100-centering routine. Three standard reflections ($\bar{2}\bar{7}3$; $\bar{2}9\bar{1}$; $29\bar{1}$) were measured every 2 h to check the stability and orientation of the crystal; no significant variations were detected. The structure was refined as described above using anisotropic temperature factors for Pt, W and P atoms and isotropic factors for the others. Upon convergence the possible presence of peaks due to the hydrides was checked using Fourier difference maps calculated with a limited data set (cut off: $\sin\theta/\lambda$ 0.33 $Å^{-1}$) [17]: no significant peaks above the background were detected. An attempt was therefore made to indirectly locate the hydrides by minimizing the potential energy using Orpen's HYDEX [10] program. Two energy minima (one for a terminal and one for a bridging position) were found, in keeping with the NMR results. The $M-H_b$ distances (1.80 Å) are constrained by the minimization procedure to be equal. The $W-H_{term}$ distance is 1.77 Å. An attempt to include these atoms in the refinement gave unacceptable positional and thermal parameters and was not pursued further. During refinement the hydrogen atoms on carbon in their calculated positions (C–H 0.95 Å) were taken into account but not refined. Final positional parameters are listed in Table 5.

Structural study of [10][BPh$_4$]

Crystals of [**10**][BPh_4] are elongated prisms and are air-stable. A crystal of approximate dimensions 0.13 × 0.16 × 0.32 mm was chosen for data collection and

mounted on a glass fiber at a random orientation. Cell constants were obtained by least squares fit of 25 high order reflections on the diffractometer. Three standard reflections ($6\bar{1}2$; $61\bar{2}$; 612), measured every 2 h, were used to monitor data collection: no significant variations due to decay of the crystal or instability of the experimental apparatus were detected. The structure was refined as previously described. Upon convergence, the final Fourier difference map showed two peaks between the two metal in acceptable positions for the μ-H atoms. Their presence was confirmed by calculating a Fourier difference map with a limited data set (as above) and by their indirect location by means of the program HYDEX. Two energy minima were found in positions similar to those on the Fourier map. The HYDEX program, which constrains the Pt–H distance to be equal to W–H, gives Pt–H 1.80 Å. These atoms were included in the refined model but their positions converged to give unacceptable M–H distances and therefore were not retained in the final model. The contribution of the H atoms bonded to the carbons, kept fixed in their idealized positions (C–H 0.95 Å), was taken into account during the refinement. Final positional parameters are given in Table 6.

Supplementary material: Tables of observed and calculated structure factors, thermal factors, and a complete list of bond lengths and angles for compounds **7**[BPh_4] and **10**[BPh_4] may be obtained from the authors on request.

Acknowledgements

This work was supported by the Ministero della Pubblica Istruzione (A.A.) and the Swiss National Science Foundation (A.T.). R.N. carried out the work with the support of the Exchange Programme Swiss National Science Foundation/Consiglio Nazionale delle Ricerche.

References

1 H.C. Clark, P.L. Fiess and C.S. Wong, Can. J. Chem., 55 (1977) 177.
2 L.M. Venanzi, Coord. Chem. Revs., 43 (1982) 251, and ref. quoted therein.
3 M.L.H. Green and P.J. Knowles, J. Chem. Soc., Perkin Trans., 1 (1973) 989.
4 (a) J.W. Lauher and R. Hoffmann, J. Am. Chem. Soc., 98 (1976) 1729; (b) M.L.H. Green, Pure Appl. Chem., 30 (1972) 373.
5 A. Albinati, R. Naegeli, A. Togni and L.M. Venanzi, Organometallics, 2 (1983) 926.
6 M.L.H. Green, J.A. McCleverty, L. Pratt and G. Wilkinson, J. Chem. Soc., (1961) 4854.
7 R. Usón, J. Fornies, P. Expinet and M.P. Garcia, Rev. Acad. Cienc. Exactas, Fis.-Quim. Nat. Zaragoza, 32 (1977) 193.
8 J. Chatt and R.G. Wilkins, J. Chem. Soc., (1951) 273.
9 International Tables for X-Ray Crystallography, Kynoch Press, Birmingham, 1974, vol. IV.
10 A.G. Orpen, J. Chem. Soc., Dalton Trans., (1980) 2509.
11 B. Deubzer and H.D. Kaesz, J. Am. Chem. Soc., 90 (1968) 3276.
12 F. Bachechi, G. Bracher, D.M. Grove, B. Kellenberger, P.S. Pregosin, L.M. Venanzi and L. Zambonalli, Inorg. Chem., 22 (1983) 1031.
13 D. Carmona, R. Thouvenot, L.M. Venanzi, F. Bachechi and L. Zambonelli, J. Organomet. Chem., 250 (1983) 589.
14 N.W. Alcock, O.W. Howarth, P. Moore and G.E. Morris, J. Chem. Soc., Chem. Comm., (1979) 1160.
15 A. Albinati, A. Togni and L.M. Venanzi, Organometallics, 5 (1986) 1785.
16 A. Albinati, T.J. Emge, T.F. Koetzle, S.V. Meille, A. Musco and L.M. Venanzi, Inorg. Chem., 25 (1986) 4821.
17 R.G. Teller and R. Bau, Structure and Bonding (Berlin), 44 (1981) 1.

18 G.W. Parshall, Inorg. Synth., 12 (1972) 28.
19 T. Yoshida, T. Matsuda and S. Otsuka, Inorg. Synth., 19 (1979) 108.
20 F.R. Hartley, The Chemistry of Platinum and Palladium, Applied Science, Publ., London, 1973, p. 460.
21 G.W. Parshall, J. Am. Chem. Soc., 96 (1974) 2360.
22 D.W.J. Cruickshank, in A. Ahmed (Ed.), Computing Methods in Crystallography, Munksgaard, Copenhagen, 1972.
23 B.T.M. Willis and A.W. Prior, Thermal Vibrations in Crystallography, Cambridge University Press, Cambridge, 1975, p. 101.